

Supporting Information for “Constructing a 3-D radially anisotropic crustal velocity model for Oklahoma using full waveform inversion”

Shuo Zhang¹ and Hejun Zhu^{1,2}

¹Department of Geosciences, the University of Texas at Dallas

²Department of Physics, the University of Texas at Dallas

Contents of this file

1. Text S1 to S2
2. Figures S1 to S6

Introduction

In this supporting document, we provide additional details on data processing and analysis to support discussions in the main text. Section S1 provides waveform comparisons based on different velocity models. Section S2 provides checkerboard test results with respect to α_h , α_v , and β_h .

Text S1. Comparison between observed and predicted seismic recordings based on different velocity models

We show predicted seismograms based on the initial model to illustrate the improvement of data fitting by the inversion (Figure S1). Using the same earthquake and seismic arrays

as shown in Figure 2 of the main text, we observe the reduction of time shifts between observed and predicted recordings.

As a comparison, we also simulate seismic recordings based on the 1-D OGS velocity profile (Figure S2), with the same earthquake and station arrays in Figure S1. Compared with Figure 2 in the main text, larger mismatches in waveform fitting in Figure S2, especially for large epicentral distances, indicate the performance of the inverted 3-D velocity model.

Text S2. Checkerboard tests

A checkerboard model is designed with positive and negative Gaussian-shape anomalies (Figure S3), with the standard deviation $\sigma_h = 30km$ and $\sigma_v = 10km$. The magnitude of the checkerboard model is set to be 14% of the maximal value of the corresponding model parameters. Considering the interreaction among different model parameters, four individual tests are performed for α_h , α_v , β_h and β_v , respectively. To recover the checkerboard pattern, two synthetic seismograms are generated by the original and perturbed models, which are then used to compute misfit gradients. The subtraction of these two gradients is used to approximate the pattern of the Hessian on specific model parameters. Other than Figure 8 with respect to β_v in the main text, Figures S4, S5 and S6 show the recovered checkerboard patterns for α_h , α_v , and β_h . Similar to Figure 8 in the main text, the recovered perturbations involve the positive/negative anomalies in the horizontal direction, with imperfect Gaussian shapes which are determined by the ray sampling. Vertically, the current acquisition system can detect velocity anomalies at depths shallower than 40 km. Except for the resolution assessment, the checkerboard test can also be used to evaluate trade-offs among different model parameters. In these four experiments, the

contamination among model parameters is limited, although we can still observe leakages among model parameters. The magnitude of the perturbation in unperturbed model parameters is ten times smaller than that in the perturbed parameter. These checkerboard tests validate model parameterization and model resolution in this study.

References

- Johnson, K. S. (1973). Oklahoma geological survey. *Annual Review, Indiana,*” in *Mining*.
- Marsh, S., & Holland, A. (2016). Comprehensive fault database and interpretive fault map of oklahoma. *Oklahoma Geol. Surv. Open-File Rep. OF2-2016, Oklahoma Geological Survey, Norman, OK*.
- Zhu, H. (2018). Crustal wave speed structure of north texas and oklahoma based on ambient noise cross-correlation functions and adjoint tomography. *Geophysical Journal International*, 214(1), 716–730.

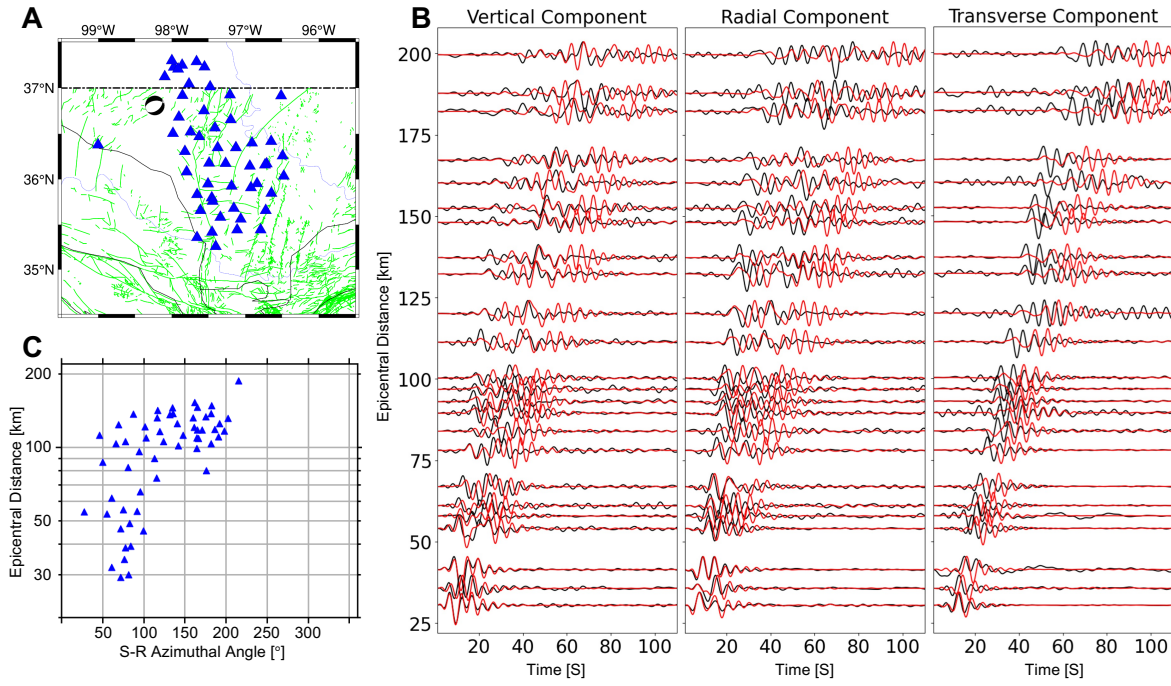


Figure S1. Performance of the initial velocity model in data domain. The locations of the particular earthquake and corresponding stations are shown in panel A, with the distribution of azimuthal and epicentral distance shown in panel C. Panel B shows the comparison between observed (black) and predicted (red) seismograms based on the initial velocity model (Zhu, 2018) within a 5-30 s passband. Green lines in panel A are fault traces measured at the Earth's surface (Marsh & Holland, 2016), and the thin black lines denote the boundaries of geological provinces in Oklahoma (Johnson, 1973)

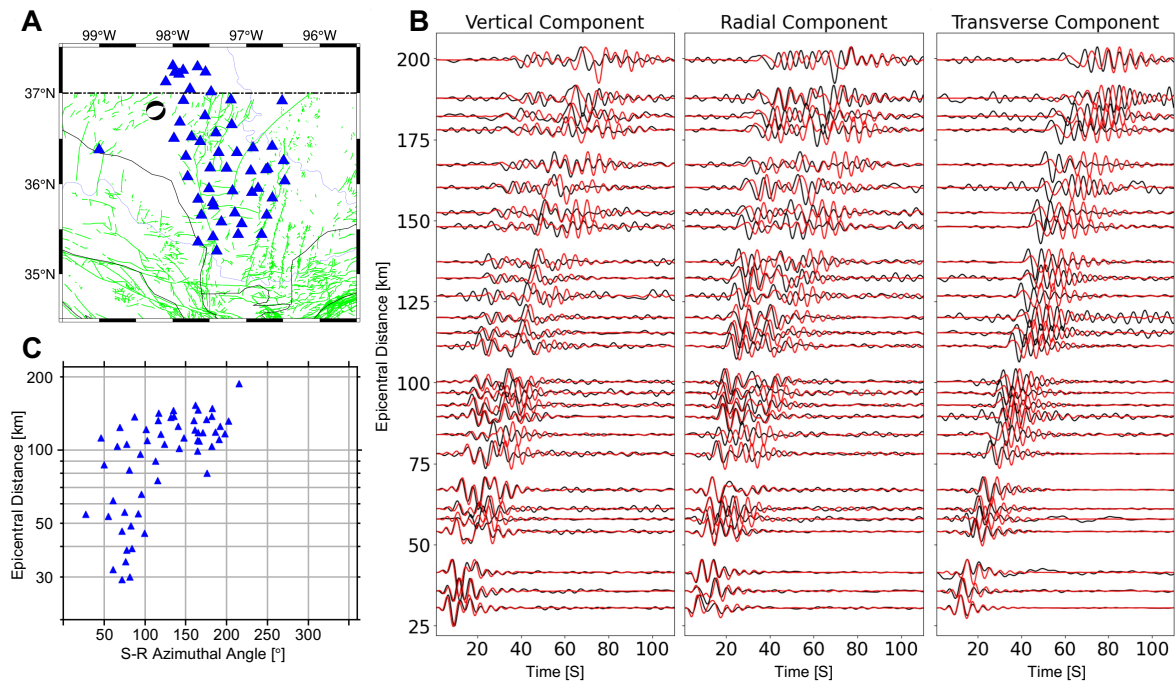


Figure S2. The same settings as Figure S1 but from simulations based on OGS-1D velocity profile.

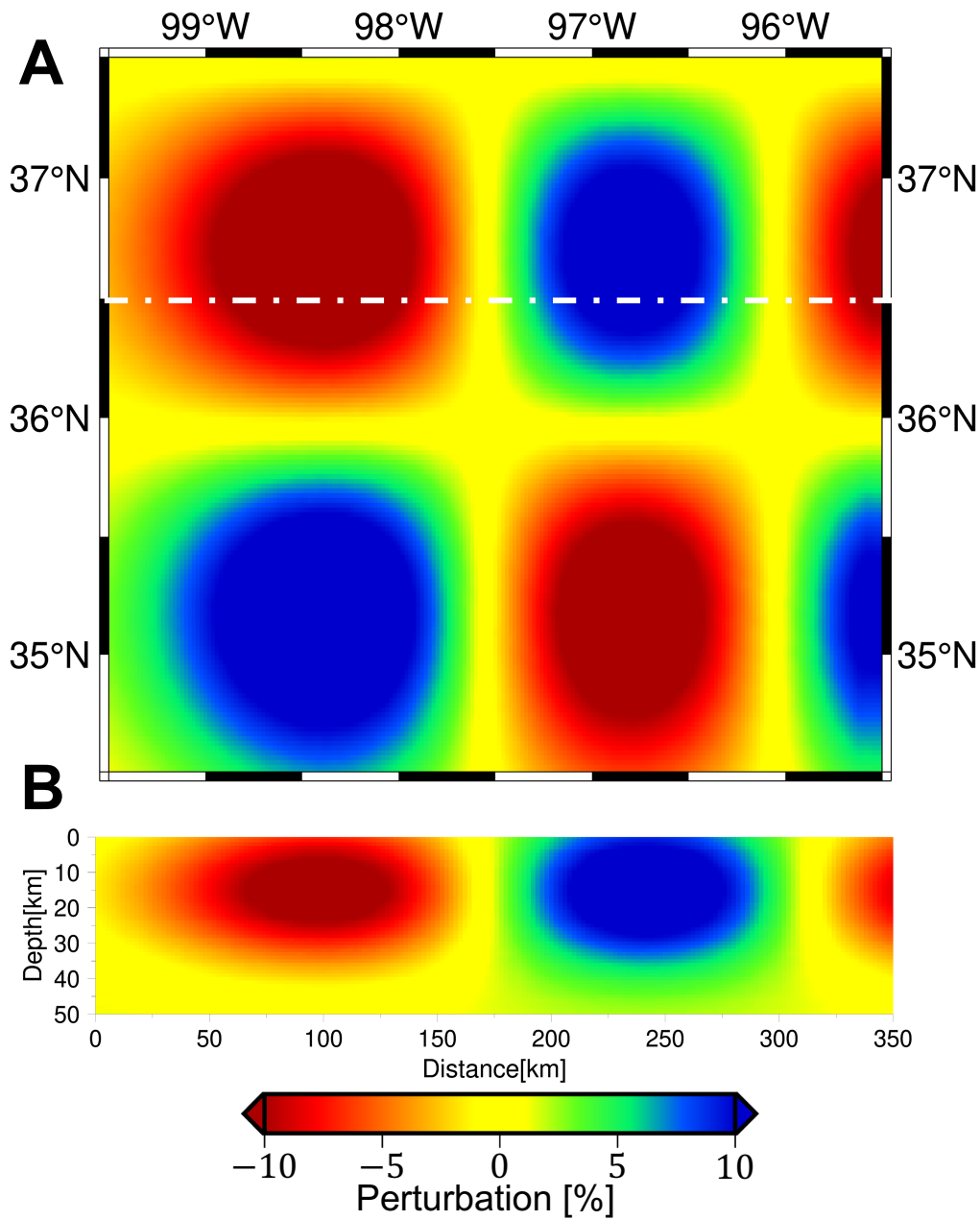


Figure S3. A designed Checkerboard model. Several positive and negative Gaussian-shape anomalies are distributed laterally in Panel A. A vertical section is cut along the white dashed line in panel A and shown in Panel B. The standard deviations of these Gaussian anomalies are $\sigma_h = 30km$ in the horizontal direction, and $\sigma_v = 10km$ in the vertical direction.

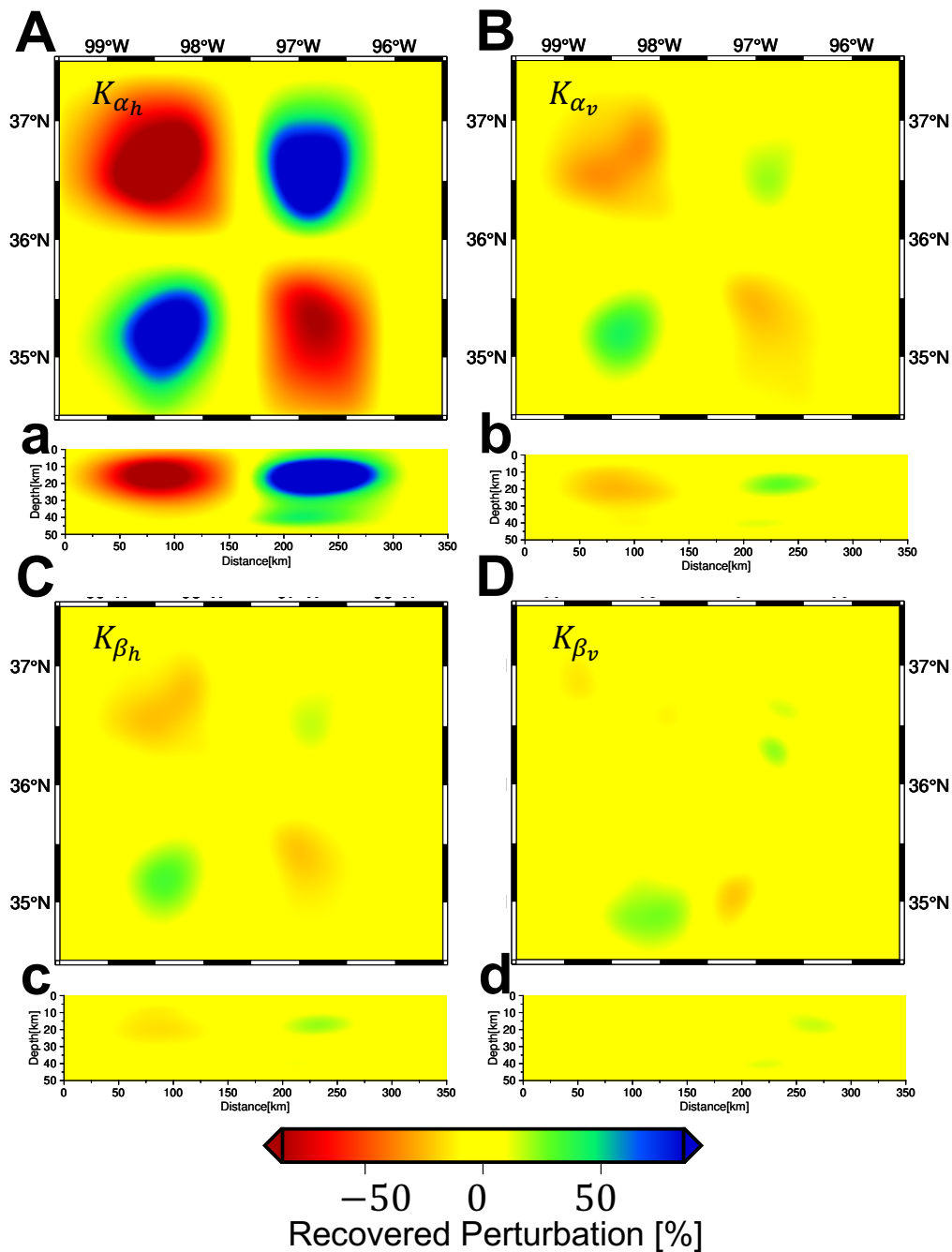


Figure S4. Recovered model gradients with respect to the model perturbation on α_h . Panel A, B, C and D are the horizontal cross section of K_{α_h} , K_{α_v} , K_{β_h} and K_{β_v} , respectively. Panel a, b, c, and d are the vertical sections of panels A, B, C and D. To make it comparable, K_{α_h} , K_{α_v} , K_{β_h} , and K_{β_v} are normalized by the maximum magnitude of K_{α_h}

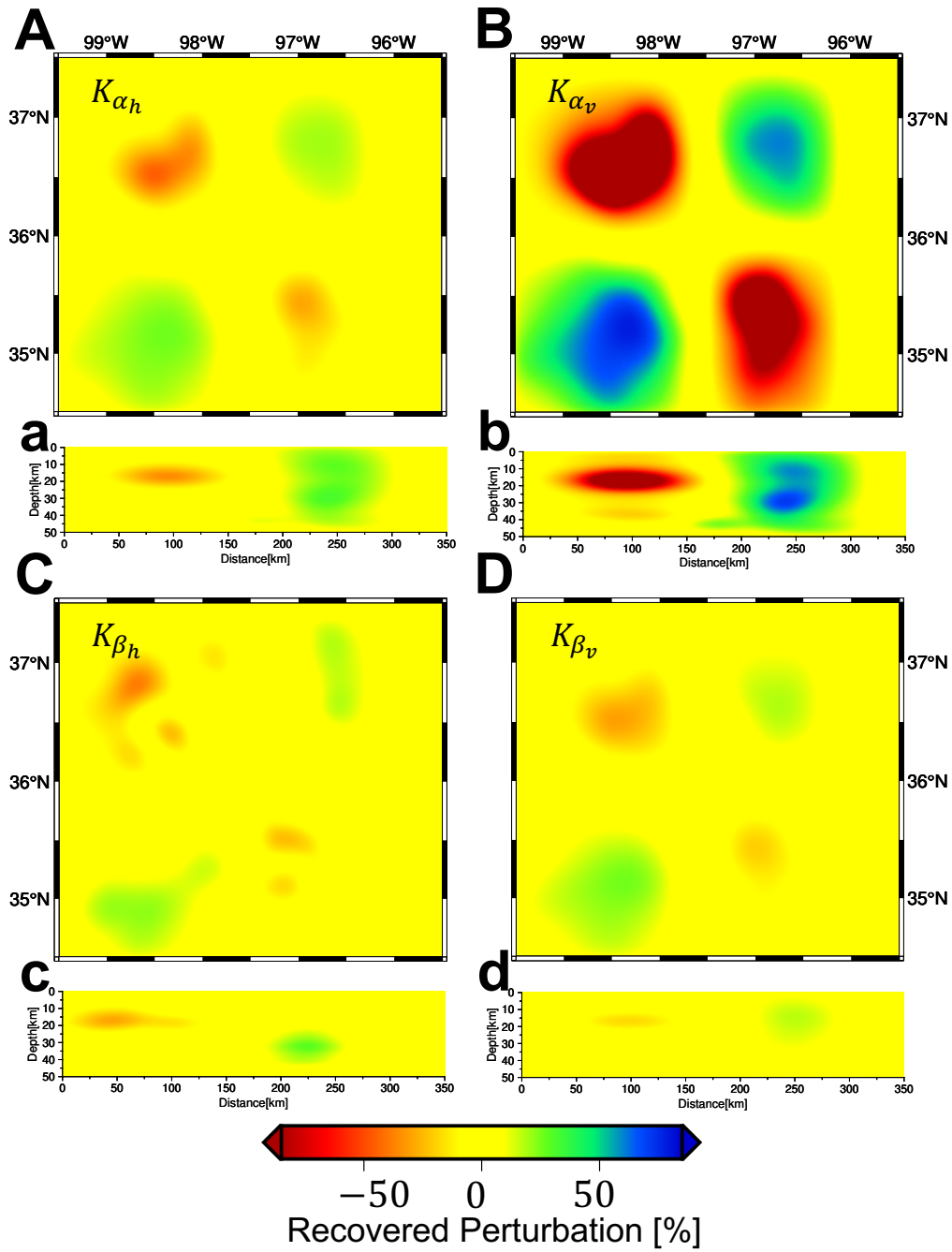


Figure S5. The same settings as Figure S4 but for K_{α_v}

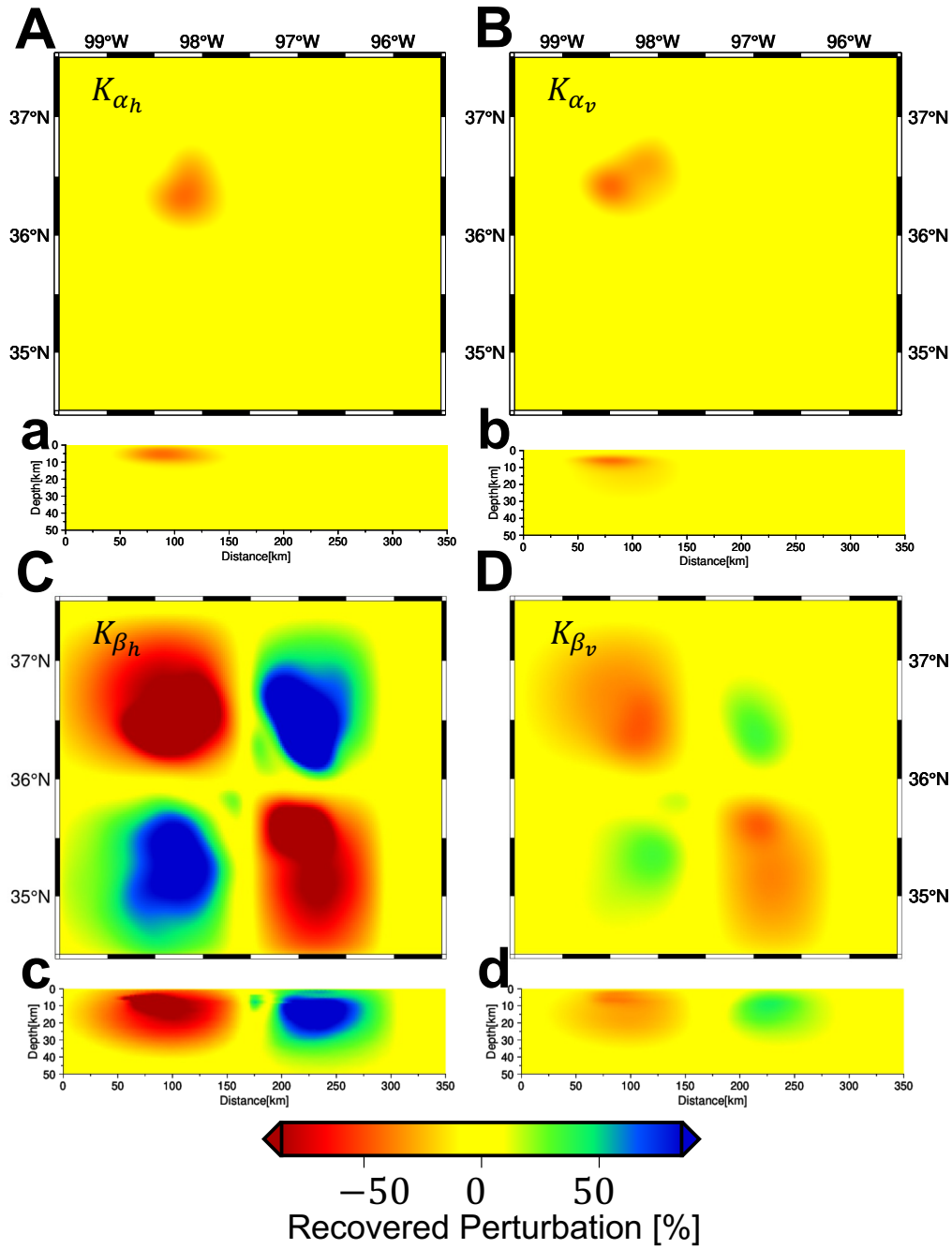


Figure S6. The same settings as Figure S4 but for K_{β_h}

April 28, 2023, 1:27am